Theoretical Studies of Inorganic and Organometallic Reaction Mechanisms. 17. Unprecedented C−C Bond Activation at Rhodium(I) and Iridium(I)

Zexing Cao† and Michael B. Hall*

Department of Chemistry, Texas A&M University, College Station, Texas 77843

Received December 20, 1999

Activation of C−C and C−H bonds by the Rh(I) and Ir(I) complexes (PCP)MCl (M = Rh, Ir; PCP = $C_6H_3(CH_3)(CH_2PH_2)_2$) has been studied by density functional methodology. C−H activation from either of the three-coordinate intermediates **1a** and **1b** has a high barrier (>25 kcal/mol). Direct C−C activation does not occur from either **1a** or **1b** because the C−C bond is sterically inaccessible. Plausible C−C and C−H activation mechanisms under mild conditions are related to four-coordinate η^1-arene intermediates, **3a** or **3b**, which are formed prior to the activation processes. Activation energies for the direct C−C oxidative addition at Rh(I) and Ir(I) were calculated to be 14.3 and 12.6 kcal/mol, respectively. The C−C bond activation products form with an exothermicity of −4.4 and −24.1 kcal/mol relative to the η^1-arene intermediates **3a** and **3b**, respectively. The unexpected reactivity for C−C activation in PCP ligand systems can be ascribed to the formation of the η^1-arene intermediates and the existence of strong Ar−metal bonds in transition states for C−C bond activation. The former makes the C−C bond accessible to the metal center, and the latter significantly reduces the barrier of the C−C activation process. "Solvent" coordination also stabilizes the C−C activation product more than the C−H activation product.

I. Introduction

Activation of C−C and C−H bonds at transition-metal centers is of fundamental importance in organometallic, biological, and industrial chemistry. While much experimental effort has been devoted to the exploration of metal insertion into C−H bonds,[1−3] direct C−C bond oxidative addition is relatively rare because the substantially higher barrier for activation makes it much less favorable than C−H bond cleavage.[4,5] Metal-promoted C−C activation under homogeneous conditions has become a prominent challenge in recent years.

Two classes of C−C activation reactions have been relatively well-documented. First, metal insertion is observed in systems with strained C−C bonds,[6] and second, C−C bonds are cleaved through C−H activation followed by β-alkyl transfer.[7] Thermodynamic and kinetic driving forces for C−C activation in strained systems have been ascribed to strain relief in both the product and the transition state. In part, these driving forces arise from the phase adaptation of interacting frontier d_σ ($d^x s^y p^z$ hybrid) and d_π orbitals of the transition metal with σ_{C-C} and σ^*_{C-C} orbitals in the strained systems. Recently, Bergman and co-workers observed reversible β-methyl elimination/migratory insertion at ruthenium(II) for the first time.[7e] The activation energy for the β-methyl migratory insertion was determined to be 26.0 ± 1.2 kcal/mol.

Direct metal insertion into a strong, unstrained C−C bond is rare.[8] Recently, Milstein and co-workers[9] observed that Rh and Ir insertion into the unstrained C−C bonds of Ar−CH_3, Ar−CH_2CH_3, and Ar−CF_3 in the

† Permanent address: Department of Chemistry, Xiamen University, Xiamen 361005, China.

(1) (a) Hill, C. L. *Activation and Functionalization of Alkanes*; Wiley: New York, 1989. (b) Ryabov, A. D. *Chem. Rev.* **1990**, *90*, 403. (c) Jones, W. D.; Feher, F. J. *Acc. Chem. Res.* **1989**, *22*, 91. (d) Davies, J. A.; Watson, P. L.; Liebman, J. F.; Greenberg, A. *Selective Hydrocarbon Activation, Principles and Progress*; VCH: New York, 1990. (e) Crabtree, R. H. *Chem. Rev.* **1985**, *85*, 245. (f) Crabtree, R. H. *The Organometallic Chemistry of the Transition Metals*; Wiley: New York, 1988. (g) Crabtree, R. H. *Angew. Chem., Int. Ed. Engl.* **1993**, *32*, 789.

(2) (a) Bergman, R. G. *Science* **1984**, *223*, 902. (b) Burger, P.; Bergman, R. G. *J. Am. Chem. Soc.* **1993**, *115*, 10462. (c) Arndtsen, B. A.; Bergman, R. G.; Mobley, T. A.; Peterson, T. H. *Acc. Chem. Res.* **1995**, *28*, 154. (d) Arndsten, B. A.; Bergman, R. G. *Science* **1995**, *270*, 1970.

(3) Lohrenz, J. C. W.; Hacobsen, H. *Angew. Chem., Int. Ed. Engl.* **1996**, *35*, 1305.

(4) (a) Rybtchinski, B.; Milstein, D. *Angew. Chem., Int. Ed.* **1999**, *38*, 870. (b) Gozin, M.; Aizenberg, M.; Liou, A.; Weisman, A. Ben-David, Y.; Milstein, D. *Nature* **1994**, *370*, 42. (c) Gozin, M.; Weisman, A.; Ben-David, Y.; Milstein, D. *Nature* **1993**, *364*, 699.

(5) (a) Murakami, M.; Amil, H.; Ito, Y. *Nature* **1994**, *370*, 540. (b) Jun, C.; Lee, H. *J. Am. Chem. Soc.* **1999**, *121*, 880.

(6) (a) Periana, R. A.; Bergman, R. G. *J. Am. Chem. Soc.* **1986**, *108*, 7346. (b) Periana, R. A.; Bergman, R. G. *J. Am. Chem. Soc.* **1984**, *106*, 7272. (c) Shaltout, R. M.; Sygula, R.; Sygula, A.; Fronczek, F. R.; Stanley, G. G.; Rabideau, P. W. *J. Am. Chem. Soc.* **1998**, *120*, 835. (d) Flood, T.; Statler, J. A. *Organometallics* **1984**, *3*, 1795. (e) Cassar, L.; Eaton, P. E.; Halpern, J. *J. Am. Chem. Soc.* **1970**, *92*, 3515. (f) Bishop, K. C. *Chem. Rev.* **1976**, *76*, 461. (g) Jennings, P. W.; Johnson, L. L. *Chem. Rev.* **1994**, *94*, 2241.

(7) (a) Corker, J.; Lefebvre, F.; Lecuyer, C.; Dufaud, V.; Quignard, F.; Choplin, A.; Evans, J.; Basset, J. M. *Science* **1996**, *271*, 966. (b) Watson, P. L.; Parshall, G. W. *Acc. Chem. Res.* **1985**, *18*, 51. Jun, C.-H. *Organometallics* **1996**, *15*, 895. (c) Hartwig, J. F.; Bergman, R. G.; Anderson, R. A. *Organometallics* **1991**, *10*, 3344. (d) McNeill, K.; Anderson, R. A.; Bergman, R. G. *J. Am. Chem. Soc.* **1995**, *117*, 3625. (e) McNeil, K.; Anderson, R. A.; Bergman, R. G. *J. Am. Chem. Soc.* **1997**, *119*, 11244.

(8) (a) van Koten, G.; Timmer, K.; Noltes, J. G.; Spek, A. L. *J. Chem. Soc., Chem. Commun.* **1978**, 250. (b) Grove, D. M.; van Koten, G.; Louwen, J. N.; Noltes, J. G.; Spek, A. L.; Ubbels, H. J. C. *J. Am. Chem. Soc.* **1982**, *104*, 6609. (c) Canty, A. J.; van Koten, G. *Acc. Chem. Res.* **1995**, *28*, 406. (d) Albrecht, M.; Gossage, R. A.; Spek, A. L.; van Koten, G. *J. Am. Chem. Soc.* **1999**, *121*, 11898.

10.1021/om991015c CCC: $19.00
Publication on Web 07/22/2000

Scheme 1

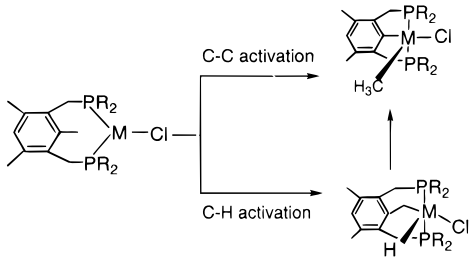

^{t}Bu-PCP ligand systems is not only thermodynamically but also kinetically preferred over the competing insertion into the C−H bonds. The C−H and C−C activation processes appear to take place independently and concurrently. The C−H activation product in the Rh−PCP system can be converted into the C−C activation product at room temperature, while this conversion in the Ir−PCP system occurs only at 100 °C. An unsaturated three-coordinate intermediate, M(DTBPM)Cl (M = Rh, Ir; DTBPM = 1,3-$(CH_2P(t\text{-}Bu)_2)_2$-2,4,6-$(CH_3)_3C_6H$), is presumed to be involved in the C−C and C−H activation processes (Scheme 1). Furthermore, the specific orientation of the key metal orbitals toward the C−C bond being activated in the three-coordinate intermediate is thought to account for the preference of C−C bond activation.

Numerous theoretical calculations have been directed at C−H bond activation, while calculations of C−C bond cleavage are relatively scarce.[10−16] Generally, metal insertion into a C−H bond is kinetically favored over metal insertion into a C−C bond because of substantially higher activation energy for the latter. Theoretical calculations on C−H and C−C bond activation by bare transition-metal atoms show that the barriers to insertion of late first-transition-row metals into the C−C bond of ethane and the C−H bond of methane are 40−45 and 20−25 kcal/mol, respectively, while late second-transition-row metals have substantially lower barriers, 13−27 and 0−9 kcal/mol, respectively.[13] Similar differences in the reactivity of C−C and C−H bond activation were also observed experimentally in reactions involving bare transition-metal ions M^+.[17−19] In the direct reaction of Fe^+ with propane, the activation barrier for the C−H bond insertion (∼11 kcal/mol) is substantially lower than that of the C−C activation (∼20 kcal/mol).[20] Product kinetic energy release distributions (KERDs) for reactions of Fe^+, Co^+, and Ni^+ with acetone suggest that the transition state for C−C bond activation in small alkanes is 6 ± 5 kcal/mol higher in energy than that for C−H bond activation.[18a]

In theoretical calculations on transition-metal complexes relatively low activation energies for C−H bond activation are predicted.[10−12,15,16] For instance, the C−H oxidative addition of CH_4 to unsaturated CpML (Cp = η^5-C_5H_5; M = Rh, Ir; L = CO, PR_3) complexes has a low barrier of 2−9 kcal/mol according to DFT calculations by Ziegler et al.[11b] and MP2 calculations by Hall and co-workers[15a,b,i] and by Musaev and Morokuma.[10b] More recently, Niu and Hall studied the inter- and intramolecular C−H activation in the cationic iridium(III) complex $CpIr(PMe_3)CH_3^+$.[15c] They found that the intermolecular C−H activation process has a low barrier of 9.6 kcal/mol at the B3LYP level, in spite of the fact that the product is an unstable Ir(V) intermediate.

In this work, we employ density function theory (DFT) to explore the mechanistic aspects of the unprecedented C−C activation observed at rhodium(I) and iridium(I) centers by Milstein and co-workers.[9] Optimized geometries and energies of intermediates, transition states, and products along possible reaction paths provide insight into the origin and mechanism of this facile C−C activation.

II. Computational Details

Effective core potentials (ECP) were used to replace the 28 and 60 innermost electrons of the Rh and Ir atoms, respectively, as well as [Ne] cores of the P and Cl atoms.[21] The outermost 5p and 6p valence orbitals for the ECP basis sets of Rh and Ir atoms, respectively, have been replaced by the optimized (41) split basis sets from Couty and Hall.[22] The ECP basis sets of P and Cl are augmented by adding d-polarization functions.[23] For the two C atoms and the three H atoms

(9) (a) Rybtchinski, B.; Vigalok, A.; Ben-David, Y.; Milstein, D. *J. Am. Chem. Soc.* **1996**, *118*, 12406. (b) van der Boom, M. E.; Liou, S.-Y.; Ben-David, Y.; Gozin, M.; Milstein, D. *J. Am. Chem. Soc.* **1998**, *120*, 13415. (c) van der Boom, M. E.; Ben-David, Y.; Milstein, D. *J. Am. Chem. Soc.* **1999**, *121*, 6652. (d) Rybtchinski, B.; Milstein, D. *Angew. Chem., Int. Ed.* **1999**, *38*, 870.

(10) (a) Koga, K.; Morokuma, K. *Chem. Rev.* **1991**, *91*, 823. (b) Musaev, D. G.; Morokuma, K. *J. Am. Chem. Soc.* **1995**, *117*, 799. (c) Matsubara, T.; Koga, N.; Musaev, D. G.; Morokuma, K. *J. Am. Chem. Soc.* **1998**, *120*, 12692.

(11) (a) Cundari, T. R. *J. Am. Chem. Soc.* **1994**, *116*, 340. (b) Ziegler, T.; Tschinke, V.; Fan, L.-Y.; Becke, A. D. *J. Am. Chem. Soc.* **1989**, *111*, 9177.

(12) (a) Han, Y.-Z.; Deng, L.-Q.; Ziegler, T. *J. Am. Chem. Soc.* **1997**, *119*, 5939. (b) Ziegler, T. Chem. Rev. **1991**, *91*, 651. (c) Ziegler, T. *Can. J. Chem.* **1995**, *73*, 743.

(13) (a) Siegbahn, P. E. M.; Blomberg, M. R. A. *J. Am. Chem. Soc.* **1992**, *114*, 10549. (b) Blomberg, M. R. A.; Siegbahn, P. E. M.; Nagashima, U. Wennerberg, J. *J. Am. Chem. Soc.* **1991**, *113*, 424.

(14) (a) Low, J. J.; Goddard, W. A., III. *J. Am. Chem. Soc.* **1984**, *106*, 8321. (b) Low, J. J.; Goddard, W. A., III. *Organometallics* **1986**, *5*, 609. (c) Low, J. J.; Goddard, W. A., III. *J. Am. Chem. Soc.* **1986**, *108*, 6115.

(15) (a) Song, J.; M. B. Hall, *Organomet.* **1993**, *12*, 3118−3126. (b) Couty, M.; Bayse, C. A.; Jiménez-Cataño, R.; Hall, M. B. *J. Phys. Chem.* **1996**, *100*, 13976. (c) Niu, S.; Hall, M. B. *J. Am. Chem. Soc.* **1998**, *120*, 6169. (d) Strout, D. L.; Zaric, S.; Niu, S.; Hall, M. B. *J. Am. Chem. Soc.* **1996**, *118*, 6068. (e) Niu, S.; Strout, D. L.; Zaric, S.; Bayse, C. A.; Hall, M. B. In *Transition State Catalysis in Computational Chemistry;* ACS Symposium Series 721; Truhlar, D. G., Morokuma, K., Eds.; American Chemical Society: Washington, DC, 1999; Chapter 11, pp 138−150. (f) Niu, S.; Hall, M. B. *J. Am. Chem. Soc.* **1999**, *121*, 3992. (g) Niu, S.; Zaric, S.; Bayse, C. A.; Hall, M. B. *Organometallics* **1998**, *17*, 5139. (h) Zaric, S.; Hall, M. B. *J. Phys. Chem.* **1998**, *102*, 1963. (i) Jiménez-Cataño, R.; Hall, M. B. *Organometallics* **1996**, *15*, 1889. (j) JimÈnez-Cataño, R.; Niu, S.-Q.; Hall, M. B. *Organometallics* **1997**, *16*, 1962. (k) Niu, S.; Hall, M. B. *Chem. Rev.* **2000**, *100*, 353.

(16) Su, M.-D.; Chu, S.-Y. *J. Am. Chem. Soc.* **1997**, *119*, 5373. (b) Su, M.-D.; McDouall, J. J. W. *J. Am. Chem. Soc.* **1993**, *115*, 5768. (c) Bach, R. D.; Su, M.-D.; Aldabagh, E.; Andres, J. L.; Schlegel, H. B. *J. Am. Chem. Soc.* **1993**, *115*, 10237. Bach, R. D.; Su, M.-D. *J. Am. Chem. Soc.* **1994**, *116*, 10103.

(17) (a) Eller, K.; Schwarz, H. *Chem. Rev.* **1991**, *91*, 1121. (b) Holthausen, M. C.; Fiedler, A.; Schwarz, H.; Koch, W. *J. Phys. Chem.* **1996**, *100*, 6236.

(18) (a) Carpenter, C. J.; van Koppen, P. A. M.; Bowers, M. T. *J. Am. Chem. Soc.* **1995**, *117*, 10976. (b) van Koppen, P. A. M.; Kemper, P. R.; Bowers, M. T. *J. Am. Chem. Soc.* **1992**, *114*, 10941.

(19) Weisshaar, J. C. *Acc. Chem. Res.* **1993**, *26*, 213.

(20) Schultz, R. H.; Armentrout, P. B. *J. Am. Chem. Soc.* **1991**, *113*, 729.

(21) (a) Hay, J. P.; Wadt, W. R. *J. Chem. Phys.* **1985**, *82*, 299. (b) Hay, J. P.; Wadt, W. R. *J. Chem. Phys.* **1985**, *82*, 284.

(22) Couty, M.; Hall, M. B. *J. Comput. Chem.* **1996**, *17*, 1359.

(23) (a) Höllwarth, A.; Böhme, M.; Dapprich, S.; Ehlers, A. W.; Gobbi, A.; Jonas, V.; Köhler, K. F.; Stegmann, R.; Veldkamp, A.; Frenking, G. *Chem. Phys. Lett.* **1993**, *208*, 238. (b) Höllwarth, A.; Böhme, M.; Dapprich, S.; Ehlers, A. W.; Gobbi, A.; Jonas, V.; Köhler, K. F.; Stegmann, R.; Veldkamp, A.; Frenking, G. *Chem. Phys. Lett.* **1993**, *208*, 111.

constituting the reactive Ar_3-CH_3 group, 6-31G** basis sets are employed.[24] The standard 3-21G basis set and the STO-6G basis sets are used for other C and H atoms,[24] respectively. The above basis set is denoted as BS1. For energy calculations of relevant states BS1 was augmented by adding an f-polarization function to the Rh and Ir atoms;[23] this basis set is denoted as BS2.

For computational ease, the DTBPM ligand was modeled by 1,3-bis(phosphinomethyl)-2-methylbenzene, $C_6H_3(CH_3)(CH_2PH_2)_2$ (PCP), where hydrogen atoms were substituted for two methyl groups and four *tert*-butyl groups in actual DTBPM ligand. Comparison of theoretical calculations for models with substitution of $-P(CH_3)_2$ for $-PH_2$ show that this simplification is reasonable, although some of the steric crowding provided by the *tert*-butyl will be missing.

Intermediates, transition states, and products in C−C and C−H bond activation processes have been fully optimized by DFT calculations. The transition states and the second-order saddle point were characterized by performing vibrational frequency analysis and determining the number of imaginary frequencies. The Becke three-parameter exchange functional and the Lee−Yang−Parr correlation functional (B3LYP) are employed in all DFT calculations. MP2 and CCSD energy calculations for final products have also been performed. All theoretical calculations were carried out with GAUSSIAN 94[24] and GAUSSIAN 98[25] at the Supercomputing Facility of Texas A&M University.

III. Results and Discussion

The experimental studies by Milstein and co-workers support a mechanism in which the C−C and C−H bond activation reactions proceed from a common intermediate and the two phosphine arms of the ligands remain coordinated to the reactive metal center. Here, we describe several low-energy conformers of this intermediate, other intermediates, and transition states in the C−C and C−H activation processes.

A. C−C and C−H Bond Activation at Rhodium(I). Intermediates. Three important intermediates, **1a**, **3a**, and **5a**, are involved in the reaction (Figure 1). Intermediate **1a** is a three-coordinate complex of rhodium(I). In intermediate **3a**, the aromatic carbon atom of the $Ar-CH_3$ bond is explicitly coordinated to rhodium such that **3a** is essentially a four-coordinate η^1-arene complex. Intermediate **5a** has an agostic $Ar-CH_3\cdots Rh$ bond. At the B3LYP/BS1 level, **3a** is more stable than **1a** and **5a** by 0.3 and 1.8 kcal/mol, respectively. The profiles of the potential energy surfaces for the interconversion of these intermediates are shown in Figure 2. The B3LYP/BS1 calculations predicted a barrier of 5.7 kcal/mol for the coordination-site exchange of the chlorine ligand in **1a** through the transition state (TS) **2a**. The rotation of the methyl group in the aryl ligand of **3a** has a barrier of only 0.8 kcal/mol (TS = **4a**). Conversion from **1a** to **3a** proceeds with a barrier of 14.8 kcal/mol. In the transition state for this conversion, **7a**, one of the dative P−Rh bonds is significantly lengthened. This lengthening of a strong P−Rh bond adds significantly to the activation energy for the formation of **7a**. This barrier and large geometric change suggest that the conversion from **1a** to **3a** is not as facile as might be expected from the structures of **1a** and **3a**. In the experimental reaction systems,[9] formation of **1a** and **3a** analogues may occur early. Conversion from **3a** to **5a** proceeds via the transition state **6a** with a relatively low barrier of 4.8 kcal/mol. Both C−H and C−C bond activation can take place from **5a** with relatively low barriers (vide infra). Thus, **3a** and **5a** analogues and their equilibrium mixture are possible candidates for the observed "common intermediate".

Mechanisms and Energetics. The B3LYP/BS1 potential energy profiles of reaction paths for C−C and C−H bond activation starting from the intermediates **1a**, **3a**, and **5a** are shown in Figure 3. In intermediate **1a**, the $Ar-CH_3$ bond is far from the metal center, and the anticipated C−C bond activation cannot occur from **1a**. However, C−H bond activation can proceed directly from **1a** as depicted in Figure 3, through a relatively high barrier of 25.2 kcal/mol. Tautomerization from the initial product **9a** to the final C−H activation product **11a** proceeds with activation energy of 6.0 kcal/mol.

A striking geometric feature of intermediate **3a** is the closeness of the $Ar-CH_3$ bond to the activation center of the Rh. On the other hand, formation of the intermediate **5a** with a barrier of only 4.8 kcal/mol makes the C−H bond of $Ar-CH_3$ accessible to the Rh center. As in other C−H bond activation reactions previously reported, C−H oxidative addition to the Rh(I) intermediate **5a** to form the product **11a** has a relatively low activation energy of 3.1 kcal/mol.

In attempting to correlate both **3a** and **5a** with the initial C−C bond cleavage product **14a**, we found only one transition state, **13a**. An intrinsic reaction coordinate (IRC) search in the reverse direction from the transition state **13a** appeared to approach a geometry intermediate between **3a** and **5a**. Full geometric optimization of this intermediate geometry resulted in **5a**. These results imply that the potential surfaces involving C−C bond activation and conversion of **3a** to **5a** may be closely connected. In other words, both **3a** and **5a** may be precursors to the initial C−C activation product **14a**. Although the Ar−C bond appears to be more accessible for activation by the metal center in **3a** than it is in **5a**, where the C−C bond is farther from the metal center, the activation barrier from **5a** appears to be lower than that from **3a**. The activation energy of metal insertion into the C−C bond from **5a** to the initial product **14a**, which has an approximate symmetry plane passing through the Rh−PCP chelate core, is found to be 14.3 kcal/mol. Although the barrier for C−C activation is higher than that for the parallel C−H activation, the value is much lower than activation energies of typical C−C oxidative additions mentioned above.

(24) Frisch, M. J.; Trucks, G. W.; Schlegel, H. B.; Gill, P. M. W.; Johnson, B. G.; Robb, M. A.; Cheeseman, J. R.; Keith, T.; Petersson, G. A.; Montgomery, J. A.; Raghavachari, K.; Al-Laham, M. A.; Zakrzewski, V. G.; Ortiz, J. V.; Foresman, J. B.; Peng, C. Y.; Ayala, P. Y.; Chen, W.; Wong, M. W.; Andres, J. L.; Replogle, E. S.; Gomperts, R.; Martin, R. L.; Fox, D. J.; Binkley, J. S.; Defrees, D. J.; Baker, J.; Stewart, J. P.; Head-Gordon, M.; Gonzalez, C.; Pople, J. A. Gaussian 94, Revision B.3; Gaussian Inc., Pittsburgh, PA, 1994.

(25) Frisch, M. J.; Trucks, G. W.; Schlegel, H. B.; Scuseria, G. E.; Robb, M. A.; Cheeseman, J. R.; Zakrzewski, V. G.; Montgomery, J. A., Jr.; Stratmann, R. E.; Burant, J. C.; Dapprich, S.; Millam, J. M.; Daniels, A. D.; Kudin, K. N.; Strain, M. C.; Farkas, O.; Tomasi, J.; Barone, V.; Cossi, M.; Cammi, R.; Mennucci, B.; Pomelli, C.; Adamo, C.; Clifford, S.; Ochterski, J.; Petersson, G. A.; Ayala, P. Y.; Cui, Q.; Morokuma, K.; Malick, D. K.; Rabuck, A. D.; Raghavachari, K.; Foresman, J. B.; Cioslowski, J.; Ortiz, J. V.; Stefanov, B. B.; Liu, G.; Liashenko, A.; Piskorz, P.; Komaromi, I.; Gomperts, R.; Martin, R. L.; Fox, D. J.; Keith, T.; Al-Laham, M. A.; Peng, C. Y.; Nanayakkara, A.; Gonzalez, C.; Challacombe, M.; Gill, P. M. W.; Johnson, B. G.; Chen, W.; Wong, M. W.; Andres, J. L.; Gonzalez, C.; Head-Gordon, M.; Replogle, E. S.; Pople, J. A. Gaussian 98; Gaussian, Inc., Pittsburgh, PA, 1998.

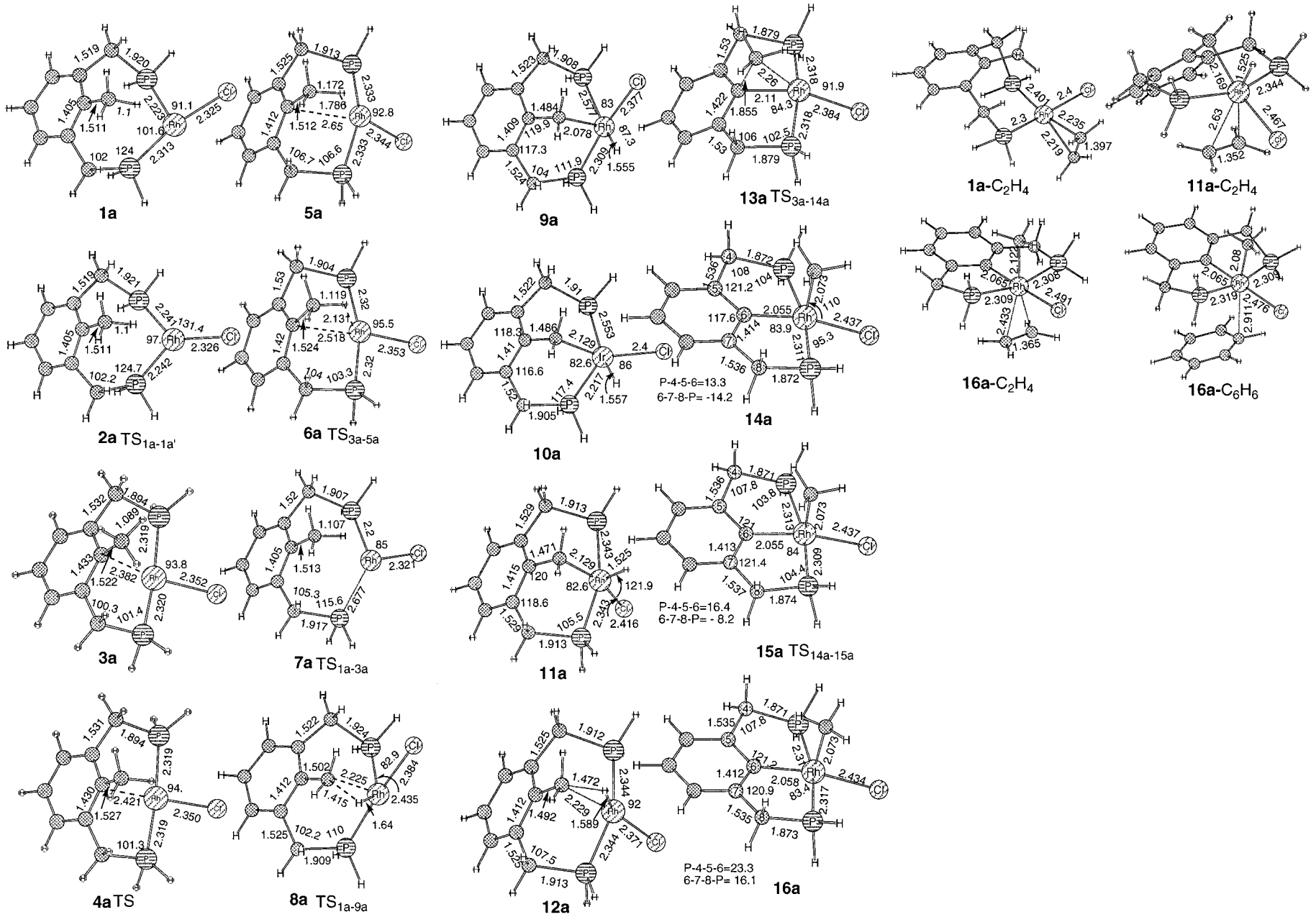

Figure 1. B3LYP optimized geometries of intermediates **1a**, **3a**, and **5a**, transition states **2a**, **4a**, **6a**, **7a**, **8a**, **10a**, **12a**, **13a**, and **15a**, products **9a**, **11a**, **14a**, and **16a**, and complexes **1a**-C_2H_4, **11a**-C_2H_4, **16a**-C_2H_4, and **16a**-C_6H_6 for the C−C and C−H activation reactions in the Rh−PCP system.

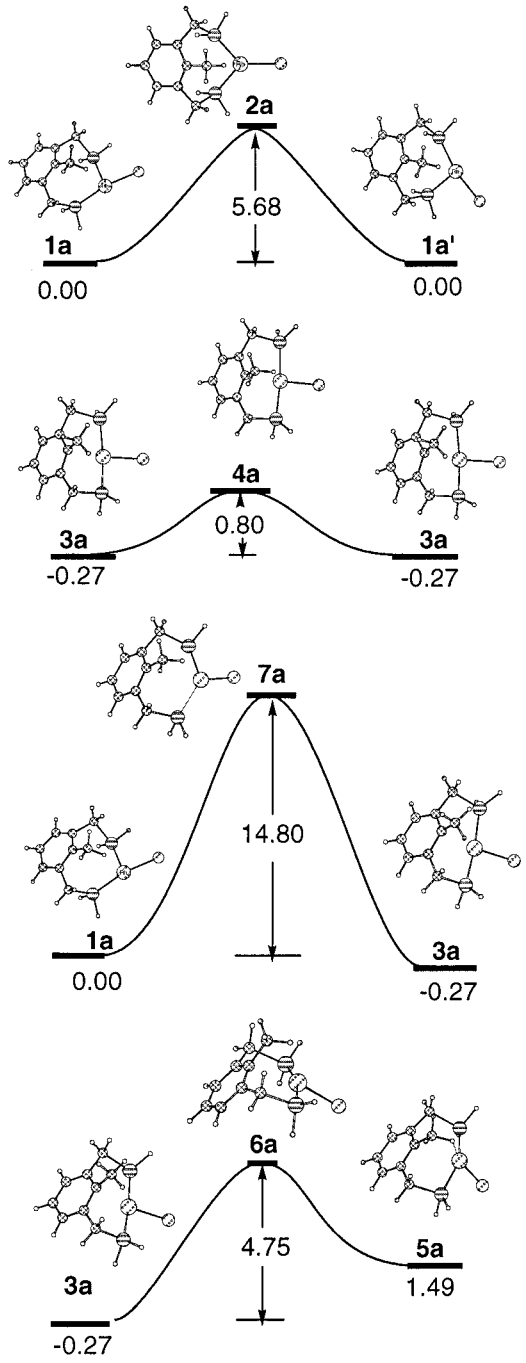

Figure 2. B3LYP potential energy profiles for the interconversion of the intermediates **1a**, **3a**, and **5a** in the Rh−PCP system (no significance should be attached to the curvature at the stationary points on these profiles).

Isomerization of **14a** to the final C−C activation product **16a** proceeds via deformation of the chelate ring (see Figure 1) with a negligible barrier (0.1 kcal/mol). The product **16a** has two inequivalent five-membered rings in the Rh−PCP chelate core, as does the experimental product, which has been characterized by an X-ray crystallographic study.[9a] Table 1 compares selected Rh-centered geometric parameters of our two C−C activation product models (−PH_2 and −PMe_2) with the X-ray structure. The calculated values for the models agree very well with those of the experiment.[9a]

At the B3LYP/BS1 level, the C−C activation product **16a** is only slightly more stable than the C−H activation product **11a**. These results imply that C−C bond activation is slightly more favorable thermodynamically than C−H activation, but the barriers suggest that it is

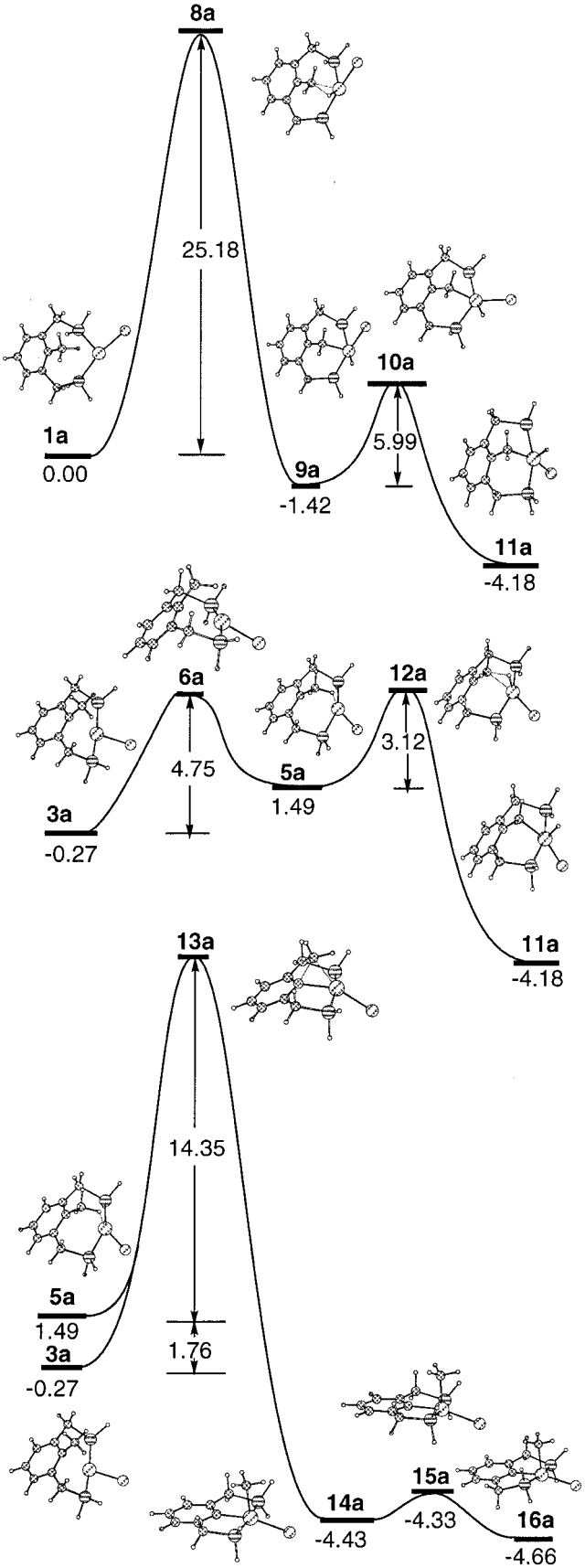

Figure 3. B3LYP potential energy profiles for the C−H and C−C activation reactions in the Rh−PCP system (no significance should be attached to the curvature at the stationary points on these profiles).

Table 1. Comparison of Selected Bond Lengths (Å) and Bond Angles (deg) for the C−C Activation Products in Rh−PCP

	calcd (**16a**)	calcd (**16a′**)[a]	exptl[b]
Rh−P	2.317	2.333	2.333(5)
	2.310	2.313	2.298(5)
Ar−Rh	2.058	2.041	2.02(2)
Rh−CH_3	2.073	2.069	2.17(2)
Rh−Cl	2.434	2.458	2.470(4)
Ar−Rh−CH_3	85.8	86.1	80.3(8)
Cl−Rh−CH_3	104.7	110.5	100.5(7)
Ar−Rh−P	83.4	84.0	83.8(5)
	83.0	82.9	82.8(5)
P−Rh−P	166.3	166.4	164.6(2)
P−Rh−Cl	95.7	96.5	95.8(2)
	95.8	94.9	97.5(2)

[a] **16a′** is derived from substitution of $-P(CH_3)_2$ for $-PH_2$ in **16a**. [b] Taken from the crystallographic structure of Rh(DTBPM)(CH_3)(Cl).[9a]

significantly less favorable kinetically. In contrast, the experimental observations suggest that the C−C bond activation is not only thermodynamically but also kinetically slightly more favorable than the C−H bond activation.[9]

To evaluate effects of the methodology and model on differences in the stability of the final activation products **16a** and **11a**, as well as on the activation energies, theoretical calculations at different levels of theory on selected models were carried out. Table 2 shows the energy differences between the C−H activation product **11a** and the C−C activation product **16a** at various levels of theory and with various models considered here. A larger basis set (B3LYP/BS2), higher level calculations (CCSD/BS1), and larger models (substitution of $-P(CH_3)_2$ for $-PH_2$) show no significant changes in the relative energies. However, the effect of a solvent molecule, such as benzene or free ethylene, as a representative alkene on the stability of **16a** relative to **11a** is remarkable. Formation of complexes of the activation products (**16a** and **11a**) with C_2H_4 and C_6H_6 stabilizes **16a** relative to **11a** by 12 and 5 kcal/mol, respectively. C_2H_4 also binds to **1a** with a binding energy of 27.2 kcal/mol in forming the complex **1a**-C_2H_4, which may be less reactive than **1a**. For **11a**, no association with C_6H_6 was observed and the "complex" **11a**-C_2H_4 is less stable by 0.8 kcal/mol than separated constituents. Although the much stronger interaction of a solvent molecule (or free ligands from initial ligand substitution reaction) with **16a** may be reduced by the steric effect of bulky phosphine ligands such as $^tBu_2P$ in the actual system, the ^{t}Bu group may act like the solvent and enhance the thermodynamic preference for C−C activation.

The geometries of **11a** and **16a** in Figure 1 show that the origin of their difference with respect to "solvent" molecules is related to their structures. The C−C activation product **16a** has a square-pyramidal geometry with an unoccupied coordination site, while the C−H activation product **11a** has an approximately trigonal-bipyramidal structure at the metal center (the H_2C−Rh−Cl bond angle is 158°), where the aryl ring blocks other ligand coordination to the Rh center. B3LYP-optimized geometries of complexes of **1a**, **11a**, and **16a** with "solvent" C_2H_4 and C_6H_6 (in one case) are also displayed in Figure 1.

B3LYP/BS2 calculations at B3LYP/BS1 geometries predict the barriers of the C−C bond activation from **3a** to **14a** and from **5a** to **14a** to be 15.9 and 14.3 kcal/mol, respectively (values similar to those with the smaller basis set). Efforts to locate solvated complexes of transition states **12a** and **13a** with C_2H_4 failed; initial complexes always decayed into separated constituents during B3LYP optimization. These results suggest that the transition states may be too crowded for solvents to play as important a role as they do in the product(s). Therefore, "solvent" or other free ligands appear not to be involved directly in C−H and C−C bond activation processes, although complexes with **3a** and **5a** may increase the effective barriers for bond activation.

Conversion between the Activation Products. All attempts to find a transition state for direct conversion from the C−H activation product **11a** to the C−C activation product **16a** were unsuccessful. A second-order saddle point with two imaginary frequencies of 959i cm^{-1} corresponding to C−H activation and 327i cm^{-1} corresponding to C−C activation was located; this result provides strong evidence that no TS connects **11a** and **16a**. Note that the barrier for the C−H reductive elimination from **11a** to **5a** is only 8.5 kcal/mol. Thus, conversion from **11a** to **16a** is most likely a two-step process, C−H reductive elimination followed by the C−C activation. The difference in thermodynamic stability between **11a** and **16a**, enhanced by solvent or free ligands, makes this conversion likely. As mentioned before, the C−C bond is accessible to the metal center in the entire domain from **3a** to **5a**, while the C−H is brought close to the metal center only through **5a**. This steric preference for C−C bond activation may balance the somewhat disadvantageous barrier. Both the conversion from **11a** to **16a** and the steric preference for C−C bond activation may explain the experimental observations where initially there appears to be more rapid formation of the C−H activation product (C−H:C−C ≈ 1.25:1), but within several hours the C−H activation product was converted into the C−C activation product.[9]

B. C−C and C−H Bond Activation at Iridium(I). Intermediates. For the Ir−PCP system, the two important low-lying intermediates **1b** and **3b** were located (see Figure 4). As in **3a**, **3b** is an η^1-arene complex with the aryl ring precoordinated to Ir. Optimization of an agostic intermediate similar to **5a** always leads to the C−H activation product **11b**. The potential energy profile for conversion from **1b** to **3b** is shown in Figure 5, where the barrier is significantly higher than the similar conversion for Rh. From the geometries of **1a**

Table 2. Energy Differences (kcal/mol) between the C−H Activation Product 11a and the C−C Activation Product 16a at Various Levels of Theory and Model

	PH_2						
	B3LYP/BS1	B3LYP/BS2	MP2/BS2	CCSD/BS1	PMe_2 B3LYP/BS1	PH_2/C_6H_6 B3LYP/BS1	PH_2/C_2H_4 B3LYP/BS1
$\Delta E_{\mathbf{11a-16a}}$	0.48	0.69	0.75	1.44	0.34	5.65	12.85

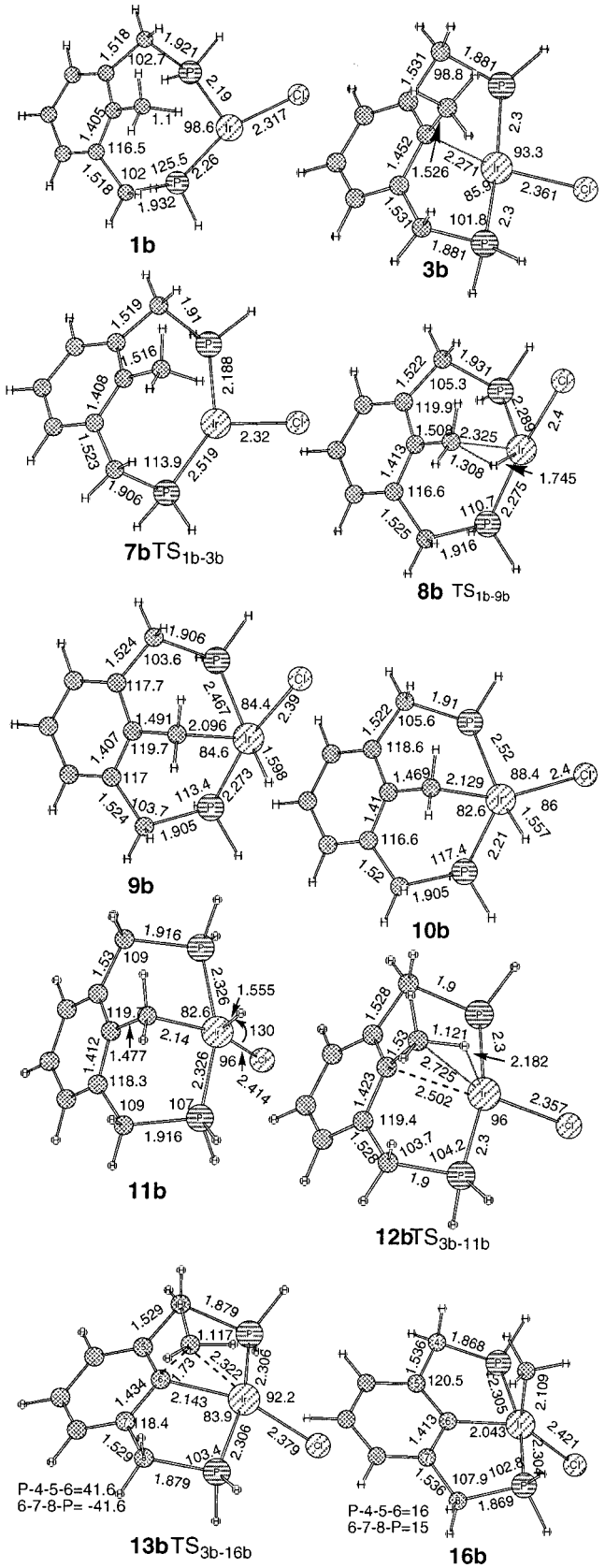

Figure 4. B3LYP optimized geometries of intermediates **1b** and **3b**, transition states **8b**, **10b**, **12b**, **13b**, and **7b**, and products **9b**, **11b**, and **16b** for the C−C and C−H activation reactions in the Ir−PCP system.

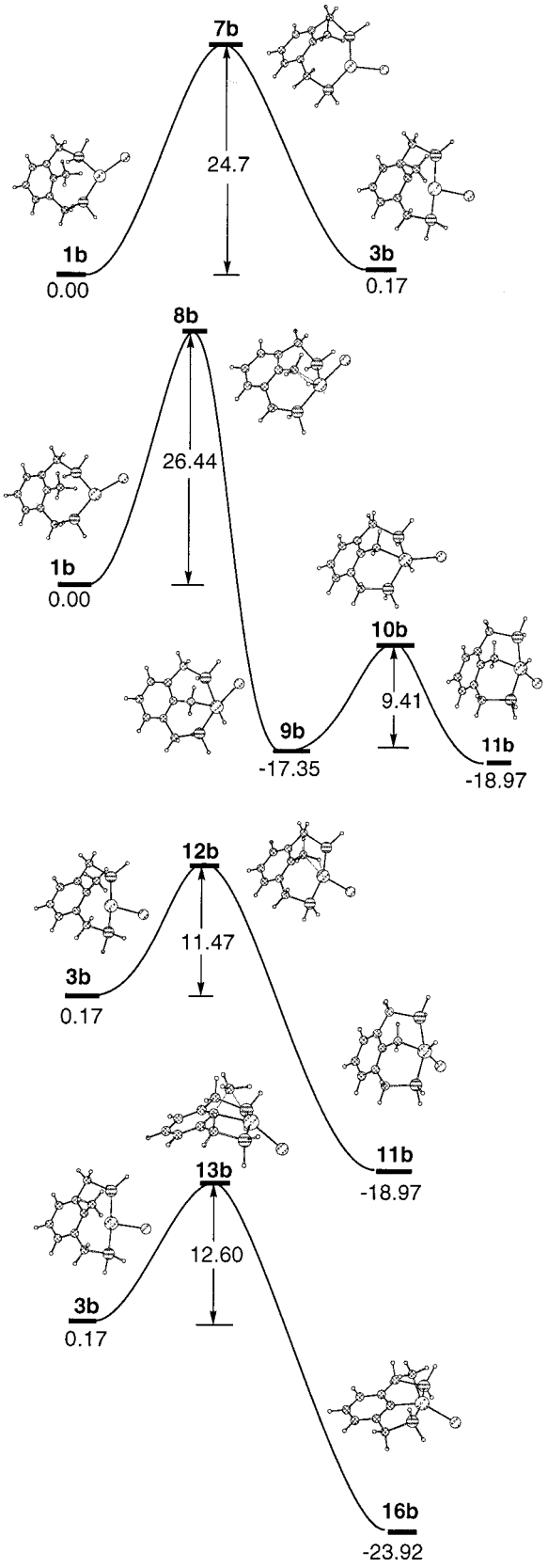

Figure 5. B3LYP potential energy profiles for the C−C and C−H activation reactions in the Ir−PCP system (no significance should be attached to the curvature at the stationary points on these profiles).

and **1b** one can see that the Ir−P bond is shorter than the Rh−P bond, suggesting that the M−P dative bond in **1b** is stronger than that in **1a**. Because of the significant M−P bond lengthening in the TS (**7a** and **7b**) the Ir system has the higher barrier. As for Rh, the two intermediates **1b** and **3b** are very close in energy,

even though there is a significant difference in their geometry.

Mechanisms and Energetics. Figure 5 also displays the potential energy profiles obtained by B3LYP/BS1 for possible reaction paths for the C−H and C−C activation processes at iridium. For the C−H activation from intermediate **1b**, the reaction proceeds to the initial product **9b** with an activation energy of 26.4 kcal/mol; subsequently, the initial product **9b** undergoes an isomerization to the final C−H activation product **11b** with a barrier of 9.4 kcal/mol. As in the case of **1a**, since the Ar−CH_3 bond is far from the Ir center in **1b**, the expected C−C bond activation does not occur from this species.

The potential energy profiles for C−H and C−C bond activation processes from the intermediate **3b** show activation energies of 11.5 and 12.6 kcal/mol, respectively. These two reactions are kinetically competitive, while C−C activation is more thermodynamically favorable than C−H activation because the C−C activation product **16b** is more stable than the C−H activation product **11b** by 4.9 kcal/mol. For the C−H and C−C reductive elimination reactions from **11b** and **16b**, the barriers are 30.4 and 46.5 kcal/mol, respectively. Thus, C−H and C−C bond activations are irreversible under mild conditions, a result which is in accordance with experiments.[9]

C. Comparison of C−H and C−C Bond Activation by Rhodium and Iridium. The direct C−H activation reactions from the intermediates **1a** and **1b** have high activation energies with similar three-center transition states. For the lowest energy reaction paths, C−H and C−C bond activation by both rhodium and iridium proceed from the two similar η^1-arene intermediates **3a** and **3b**. For the Rh−PCP system, formation of an agostic compound, **5a**, in the reaction path for C−H oxidative addition makes the structure of the three-center transition state **12a** like that expected for a late transition state. In the Ir−PCP system, which lacks a stable agostic intermediate but has a more stable product, the rather early three-center transition state **12b** with a higher barrier is predicted. Similarly, formation of the transition state **13b** for the C−C bond activation in the Ir−PCP system appears to be structurally earlier than the similar three-center transition state for the Rh−PCP system **13a**. As the C−C bond activation in Ir−PCP is more exothermic than that in Rh−PCP, no initial product like **14a** exists in the Ir−PCP reaction. The geometries of **12** and **13** in Figures 1 and 4 display the features expected for late transition states (**12a** and **13a**) in comparison with early transition states (**12b** and **13b**).

The differences in mechanisms of the C−C and C−H bond activation reactions between the Rh−PCP and Ir−PCP systems can be attributed to distinct electronic features of transition-metal centers in the common intermediates **3a** and **3b**. Previous theoretical studies of C−H bond activation suggest that a combination of donation and back-donation accounts for adduct formation and C−H bond activation, where donation from the filled σ_{C-H} orbital to the empty σ-type orbital of the metal is essential for adduct formation, and strong back-donation from the metal to the σ^*_{C-H} orbital leads to fission of the C−H bond.[15k] Thus, relatively high electron densities on the metal center are necessary for the transition metal complex to serve as a precursor for C−H and C−C bond activation. The calculated Mulliken charges on M in **3a** and **3b** are −0.08 and −0.18, respectively. The higher negative charges on Ir may account, in part, for the greater ability of **3b** to act as a bond activation precursor than **3a**. In addition, Ir−X bonds are usually stronger than the corresponding Rh−X bonds, such that bond activation by Ir is more exothermic with earlier barriers.

Scheme 2

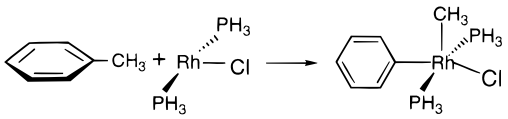

Scheme 3

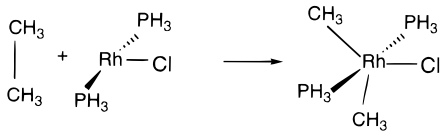

The difference in electron density can be ascribed to the distinct aryl ring precoordination to metal centers. Geometries of **3a** and **3b** (Figures 1 and 4) show that the Ar−Ir separation is shorter than the Ar−Rh separation by 0.11 Å. A stronger interaction between the aryl ring and Ir is expected to result in more negative charges on Ir in **3b**, and subsequent back-donation, which activates the C−H and C−C bonds, may occur more easily in **3b**. Stronger donation from σ_{C-H} and σ_{C-C} to Rh prior to bond activation in **3a** may be a prerequisite to the reaction. Thus, for Rh, formation of **5a** with donation from Ar−CH_3 and C−H to the metal center results in an increase of electron density on the Rh from −0.08 in **3a** to −0.20 in **5a** and makes **5a** a better precursor for subsequent C−H activation as well as C−C activation.

D. Nature of Metal-Promoted Ar−C Bond Activation. DFT calculations show that the η^1-arene complexes **3a** and **3b** are the common intermediates for both C−H and C−C activation reactions. In these η^1-arene complexes, the Ar−CH_3 bonds are brought close to the metal centers, structures which make C−C bond activation sterically accessible. The relative energies of these η^1-arene complexes reveal that this aryl ring precoordination to the metal center is weak. Presumably, the two −CH_2PH_2 arms also play an important role in the formation of these η^1-arene complexes. Existence of the η^1-arene complex provides the explanation of why Ar−CH_2CH_3 bond activation is preferred over ArCH_2−CH_3 bond activation.[9b]

We have investigated two model reactions (Schemes 2 and 3) to calibrate the effects of the η^1-arene complex and the strength of the Ar−Rh bond in the transition state. In Scheme 2, no similar η^1-arene complex was found, but an η^2-alkyl agostic complex exists. The Ar−CH_3 activation energies were calculated to be 19.0 kcal/mol relative to separated reactants and 29.1 kcal/mol relative to the η^2-alkyl agostic complex, respectively. The Ar−Rh bond length in the transition state is 2.098 Å. In Scheme 3, the C−C activation barriers are 27.1 kcal/mol relative to separated reactants and 35.6 kcal/mol relative to the η^2-alkyl agostic complex. The C−Rh bond

separation in the transition state of Scheme 3 is 2.246 Å, which is longer than the Ar−Rh separation of the transition state in Scheme 2 by 0.148 Å. Thus, the Ar−Rh bond in the TS of Scheme 2 is stronger than the C−Rh bond in the TS of Scheme 3. Compared with Scheme 3, the barrier for $Ar-CH_3$ bond activation in Scheme 2 is lower by 8.1 kcal/mol. The relatively lower activation energy for $Ar-CH_3$ bond activation in Scheme 2 can be ascribed to the existence of a strong Ar−Rh bond. Both model reactions are unlikely, in part, because the η^2-alkyl agostic interaction keeps the C−C bonds far from the metal.

These results for model reactions show that formation of the η^1-arene complexes depends on the two $-CH_2-PH_2$ arms and that the aryl ring precoordination to the metal center Rh(I) is weak despite the close approach.

E. Conclusions

The DFT calculations, described here, provide insight into the mechanism and energetics of the unprecedented C−C bond and C−H bond activation reactions in the PCP ligand systems. For the Rh−PCP system, C−C activation is thermodynamically preferred over the competing C−H activation. This thermodynamic preference may be enhanced significantly by complexation with solvent or free alkene ligand. The C−H activation product can be converted into the C−C activation product via a rapid C−H reductive elimination followed by C−C activation. The thermodynamic and steric preference of the C−C bond activation and the facile C−H reductive elimination make C−C oxidative addition preferred over C−H bond activation. For the Ir−PCP system, direct metal insertion into the C−C bond not only is thermodynamically favored but also is kinetically competitive with C−H bond oxidative addition. Furthermore, C−C and C−H bond activation processes are irreversible in the Ir−PCP system. Our calculations show that three important factors in these systems make the C−C oxidative addition favorable under mild conditions. First, formation of an approximately four-coordinate η^1-arene complex brings the C−C bond close to the activation center and makes the C−C bond accessible to the transition metal. Second, the existence of strong Ar−metal bonds in the transition state significantly lowers the activation energy. Third, specific solvent coordination at the open coordination site in the C−C bond-activation product significantly stabilizes this product. Note that for both Rh and Ir the largest (or nearly the largest) barrier in the path from **1** to both products **11** and **16** is the conversion of **1** to **3**. Thus, this step could be the rate determining step for both metals and both products.

Acknowledgment. We gratefully acknowledge the National Science Foundation (Grant No. CHE 9800184) and the Robert A. Welch Foundation (Grant No. A-648) for financial support of this work.

OM991015C